A New Electron-Transfer Donor for Photoinduced Electron Transfer in Polypyridyl Molecular Assemblies

Colleen M. Partigianoni, Sandrine Chodorowski-Kimmes, Joseph A. Treadway, Durwin Striplin, Scott A. Trammell, and Thomas J. Meyer*

Department of Chemistry, University of North Carolina at Chapel Hill, CB# 3290, Chapel Hill, North Carolina 27599-3290

Received May 14, 1998

A synthetic procedure has been devised for the preparation of the reductive quencher ligand 4-methyl-4′-(*N*-methyl-*p*-tolylaminomethyl)-2,2′-bipyridine (dmb-tol), which contains toluidine covalently bound to 2,2′-bipyridine. When bound to Re^{I} in $[Re^{I}(dmb\text{-}tol)(CO)_3Cl]$, laser flash $Re^{I} \rightarrow$ dmb metal-to-ligand charge-transfer (MLCT) excitation at 355 nm in CH_3CN at 298 ± 2 K is followed by efficient, rapid (<5 ns) appearance of a transient with an absorption feature at 470 nm. The transient spectrum is consistent with formation of the redox-separated state, $[Re^{I}(dmb^{-}\text{-}tol^{+})(CO)_3Cl]$, which returns to the ground state by back electron transfer with $k_{ET} = (1.05 \pm 0.01) \times 10^7\ s^{-1}$ ($\tau = 95 \pm 1$ ns) at 298 ± 2 K. Rapid, efficient quenching is also observed in the Ru^{II} complex $[Ru(4,4'\text{-}(C(O)NEt_2)_2bpy)_2(dmb\text{-}tol)]^{2+}$. Based on transient absorption measurements, a rapid equilibrium appears to exist between the initial metal-to-ligand charge-transfer excited state and the redox-separated state, which lies at higher energy. Decay to the ground state is dominated by back electron transfer within the redox-separated state which occurs with $k > 4 \times 10^8\ s^{-1}$ at 298 ± 2 K.

Introduction

Pyridyl and bipyridyl ligands derivatized by addition of chemically linked electron-transfer donors[1−3] and acceptors[4−6] have been used extensively in studies of photoinduced electron transfer.[1−10] Commonly used electron-transfer donors are 10-(4-picolyl)phenothiazine (py-PTZ) and 4-(10-methylphenothiazine)-4′-methyl-2,2′-bipyridine (bpy-PTZ),[1,4,9,10] in which $E_{1/2}$ for the $PTZ^{+/0}$ couple is 0.85 V vs SSCE in 1,2-dichloroethane.[10d] In $[(bpy)Re(CO)_3(py\text{-}PTZ)]^{+}$, metal-to-ligand charge transfer (MLCT), $Re^{I} \rightarrow$ bpy, excitation is followed by intramolecular

(1) (a) Chen, P.; Westmoreland, D. T.; Danielson, E.; Schanze, K. S.; Anthon, D.; Neveux, P. E.; Meyer, T. J. *Inorg. Chem.* **1987**, *26*, 1116. (b) Della, C. L.; Hamachi, I.; Meyer, T. J. *Org. Chem* **1989**, *54*, 1731. (c) Larson, S. L.; Elliott, C. M.; Kelley, D. F. *J. Phys. Chem.* **1995**, *99*, 6530. (d) Cooley, L. F.; Larson, S. L.; Elliott, C. M.; Kelley, D. F. *J. Phys. Chem.* **1991**, *95*, 10694. (e) Collin, J. P.; Guillerez, S.; Sauvage, J. P.; Barigelleti, F.; DeCola, L.; Flamigni, L.; Balzani, V. *Inorg. Chem.* **1991**, *30*, 4230.

(2) (a) Wang, Y.; Schanze, K. S. *J. Phys. Chem.* **1996**, *100*, 5408. (b) Lucia, L. A.; Wang, Y.; Nafisi, K.; Netzel, T. L.; Schanze, K. S. *J. Phys. Chem.* **1995**, *99*, 11801. (c) Wang, Y.; Hauser, B. T.; Rooney, M. M.; Burton, R. D.; Schanze, K. S. *J. Am. Chem. Soc.* **1993**, *115*, 5675. (d) MacQueen, D. B.; Schanze, K. S. *J. Am. Chem. Soc.* **1991**, *113*, 7470. (e) Perkins, T. A.; Humer, W.; Netzel, T. L.; Schanze, K. S. *J. Phys. Chem.* **1990**, *94*, 2229. (f) Schanze, K. S.; Cabana, L. A.; Netzel, T. L.; Schanze, K. S. *J. Phys. Chem.* **1990**, *94*, 2740.

(3) (a) Chodorowski-Kimmes, S.; Meyer, T. J. *Tetrahedron Lett.* **1997**, *38*, 3659. (b) Odobel, F.; Sauvage, J.-P. *New J. Chem.* **1994**, *18*, 1139. (c) Chambron, J.-C.; Coudret, C.; Sauvage, J. P. *New J. Chem.* **1992**, *16*, 361. (d) Perkins, T. A.; Hauser, B. T.; Eyler, J. R.; Schanze, K. S. *J. Phys. Chem.* **1990**, *94*, 8745.

(4) (a) Coe, B. J.; Friesen, D. A.; Thompson, D. W.; Meyer, T. J. *Inorg. Chem.* **1996**, *35*, 4575. (b) Opperman, K. A.; Mecklenburg, S. L.; Meyer, T. J. *Inorg. Chem.* **1994**, *33*, 5295. (c) Mecklenburg, S. L.; McCafferty, D. G.; Schoonover, J. R.; Peek, B. M.; Erickson, B. W.; Meyer, T. J. *Inorg. Chem.* **1994**, *33*, 2974. (d) Mecklenburg, S. L.; Peek, B. M.; Schoonover, J. R.; McCafferty, D. G.; Wall, C. G.; Erickson, B. W.; Meyer, T. J. *J. Am. Chem. Soc.* **1993**, *115*, 5479. (e) Mecklenburg, S. L.; Peek, B. M.; Erickson, B. W.; Meyer, T. J. *J. Am. Chem. Soc.* **1991**, *113*, 8540.

(5) (a) Ryu, Chong, K.; Wang, R.; Schmehl, R. H.; Ferrere, S.; Ludwikow, M.; Merkert, J. W.; Headford, C. E. L.; Elliott, C. M. *J. Am. Chem. Soc.* **1992**, *114*, 430. (b) Cooley, L. F.; Headford, C. E. L. Elliott, C. M.; Kelley, D. F. *J. Am. Chem. Soc.* **1988**, *110*, 6673. (c) Danielson, E.; Elliott, C. M.; Merkert, J. M.; Meyer, T. J. *J. Am. Chem. Soc.* **1987**, *109*, 2519. (d) Elliott, C. M.; Freitag, R. A.; Blaney, D. D. *J. Am. Chem. Soc.* **1985**, *107*, 4647.

(6) (a) Claude, J. P.; Williams, D. S.; Meyer, T. J. *J. Am. Chem. Soc.* **1996**, *118*, 9782. (b) Katz, N. E.; Mecklenburg, S. L.; Meyer, T. J. *Inorg. Chem.* **1995**, *34*, 1282. (c) Yonemoto, E. H.; Saupe, G. B.; Schmehl, R. H.; Hubig, S. M.; Riley, R. L.; Iverson, B. L.; Mallouk, T. E. *J. Am. Chem. Soc.* **1994**, *116*, 4786. (d) Goulle, V.; Harriman, A.; Lehn, J. M. *J. Chem. Soc., Chem. Commun.* **1993**, 1034. (e) Berthon, R. A.; Colbran, S. B.; Moran, G. M. *Inorg. Chim. Acta* **1993**, *204*, 3. (f) Deronzier, A.; Essakalli, M. *J. Chem. Soc., Chem. Commun.* **1990**, 242. (g) Schanze, K. S.; Sauer, K. *J. Am. Chem. Soc.* **1988**, *110*, 1180. (h) Matsuo, T.; Sakamoto, T.; Takuma, K.; Sakura, K.; Ohsako, T. *J. Phys, Chem.* **1981**, *85*, 1277.

(7) (a) Kalyanasundaram, K. *Photochemistry of Polypyridine and Porphyrin Complexes*; Academic Press: New York, 1992. (b) Sauvage, J.-P.; Collin, J.-P.; Chambron, J.-C.; Guillerez, S.; Coudret, C.; Balzani, V.; Barigelletti, F.; DeCola, L.; Flamigni, L. *Chem. Rev.* **1994**, *94*, 993. (c) Peterson, J. D.; Gahan, S. L.; Rasmussen, S. C.; Ronco, S. E. *Coord. Chem. Rev.* **1994,** *132*, 15. (d) Cabana, L. A.; Schanze, K. S. *Adv. Chem. Ser.* **1989**, *226*, 101. (e) Balzani, V.; Scandola, F. In *Photoinduced Electron-Transfer Part D, Inorganic Substrates and Applications;* Fox, M. A., Chanon, M., Eds.; Elsevier: New York, 1988; pp 148−78. (f) Schmehl, R. H.; Ryu, C. K.; Elliott, C. M.; Headford, C. L. E.; Ferrere, S. *Adv. Chem. Ser.* **1989**, *228*, 211.

(8) (a) Harriman, A.; Obodel, F.; Sauvage, J.-P. *J. Am. Chem. Soc.* **1994**, *116*, 5481. (b) Collin, J.-P.; Harriman, A.; Heitz, V.; Odobel, F.; Sauvage, J.-P. *J. Am. Chem. Soc.* **1994**, *116*, 5679.

(9) (a) Rutherford, T. J.; Keene, F. R. *Inorg. Chem.* **1997**, *36*, 2872. (b) Treadway, J. A.; Chen, P.; Rutherford, T. J.; Keene, F. R.; Meyer, T. J. *J. Phys. Chem.* **1997**, *101*, 6824. (c) Shaver, R. J.; Perkovic, M. W.; Rillema, D. P.; Woods, C. *Inorg. Chem.* **1995**, *34*, 5446. (d) Strouse, G. F.; Schoonover, J. R.; Duesing, R.; Meyer, T. J. *Inorg. Chem.* **1995**, *34*, 2725. (e) Jones, W. E., Jr.; Bignozzi, C. A.; Chen, P.; Meyer, T. J. *Inorg. Chem.* **1993**, *32*, 1167. (f) Collin, J.-P.; Guillerez, S.; Sauvage, J.-P.; Barigelleti, F.; DeCola, L.; Flamigni, L.; Balzani, V. *Inorg. Chem.* **1992**, *31*, 4112. (g) Larson, S. L.; Cooley, L. F.; Elliott, C. M.; Kelley, D. F. *J. Am. Chem. Soc.* **1992**, *114*, 9504. (h) Duesing, R.; Tapolksy, G.; Meyer, T. J. *J. Am. Chem. Soc.* **1990**, *112*, 5378.

10.1021/ic980544q CCC: $18.00
Published on Web 02/20/1999

PTZ → Re(II) electron transfer, to give the redox-separated state, $[(bpy^{-})Re(CO)_3(py\text{-}PTZ^{+})]^{+}$, which decays by $bpy^{\bullet-} \rightarrow PTZ^{\bullet+}$ back electron transfer. Assemblies of this kind have played an important role in the study of electron transfer in the inverted region,[10] and there is a continuing need for the development of new electron-transfer units for incorporation into molecular assemblies.

Schanze and co-workers have utilized aromatic amine derivatives covalently bound to pyridine.[2] As an extension of their work, we have developed a general synthetic route for covalently attaching aniline derivatives to bipyridine, which, in principle, can provide a wide range of reduction potentials by varying substituents on the aniline.[11] We report here the preparation of the first member of this series, 4-methyl-4′-(*N*-methyl-*p*-tolylaminomethyl)-2,2′-bipyridine (dmb-tol), which has a reduction potential comparable to the $PTZ^{+/0}$ couple, and its use in the study of photoinduced electron transfer.

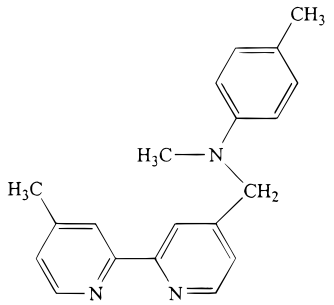

dmb-tol

Experimental Section

Materials. The ligand 4,4′-bis(diethylcarbamoyl)-2,2′-bipyridine (4,4′-$(C(O)NEt_2)_2$bpy) and the complexes [Re(dmb)$(CO)_3$Cl] and Ru-[4,4′-$(C(O)NEt_2)_2$bpy]$_2Cl_2$ were prepared as described previously.[12−14] The reagents 4,4′-dimethyl-2,2′-bipyridine (GFS Chemicals), *N*-methyltoluidine (ACROS Chemicals), BOP = 1-benzotriazoleoxy)tris-(dimethylamino)phophonium hexafluorophosphate (Nova Biochem), $Re(CO)_5Cl$ (Pressure Chemicals), NH_4PF_6 (Aldrich), and BH_3SMe_2/1.0 M in THF (Aldrich) were used as received. *N*-Methylmorpholine was purchased from Aldrich and distilled from CaH_2 prior to use. Reagent grade solvents ether, toluene, and THF, used in the preparations, were dried by distillation from Na/benzophenone under nitrogen. Spectral grade CH_3CN (Burdick & Jackson) was used for electrochemical and spectroscopic measurements. The supporting electrolyte tetra-*n*-butylammonium hexafluorophosphate (TBAH) was purchased from Aldrich and recrystallized twice from a H_2O/ethanol (2:1 v/v) mixture. Solutions for transient absorption studies were prepared by using spectral grade solvents which had been heated at reflux over and distilled from CaH_2 and then stored under vacuum over CaH_2.

Preparations. 4-Methyl-4′-(*N*-methyl-*p*-tolylaminomethyl)-2,2′-bipyridine (dmb-tol). Covalent attachment of the *N*-methyltoluidine donor to bipyridine was achieved by amide coupling of the amine followed by borane reduction. In a typical amide coupling reaction, *N*-methyltoluidine (0.55 mL, 1.2 equiv), BOP (3.0 g, 1.1 equiv), 4-carboxy-4-methyl-2,2′-bipyridine (1 g, 1 equiv), and *N*-methylmorpholine (3 mL) were combined in 50 mL of dry THF. The argon-sparged solution was stirred at room temperature for 6 h. The suspension was filtered and THF removed from the filtrate by rotary evaporation. The residue was extracted into ether and washed three times with acidic aqueous solutions at pH ∼ 5, five times with saturated aqueous $NaHCO_3$, and twice with saturated NaCl. The organic layer was dried over anhydrous $MgSO_4$ and freed of solvent by rotary evaporation. The product, 4-CH_3-4′-[C(O)N(CH_3)-*p*-$C_6H_4CH_3$]-2,2′-bipyridine, was purified by column chromatography with silica as the solid support. Excess *N*-methyltoluidine was removed by eluting with neat CH_2Cl_2, and the desired product (0.9 g) collected with 3% MeOH/CH_2Cl_2 as the eluant. The product was characterized by ^{1}H NMR in $CDCl_3$. The amide-linked toluidine shows distinguishing resonances vs TMS at 6.95 ppm (4H, m), 2.21 ppm (3H, s) and amino methyl resonances at 3.45 ppm (3H, s). Bipyridine resonances appear at 2.42 ppm (3H, s), 7.13 ppm (2H, d), 8.11 ppm (1H, s), 8.3 (1H, s), and 8.45 ppm (2H, m).

The borane reduction was carried out by using a method comparable to that previously described, but with some significant modifications.[15] The amide was dissolved in 50 mL of dried THF, and 20 mL of a 1.0 M THF solution of BH_3SMe_2 (10 equiv) was added slowly to the deaerated solution. The solution was stirred under Ar at room temperature for 72 h. Precipitation of the borane adduct of the reduced ligand was induced by slow addition of dry ether.[15c] The borane adduct was collected by filtration and then hydrolyzed to yield the free amine and boric acid by stirring in MeOH for 3 h. The methanol was completely removed in vacuo, leaving the borate acidic salt of the amine. Attempts to extract the neutral amine from basic aqueous media resulted in decomposition and poor yields. Alternatively, the acidic salt was suspended in toluene and neutralized by addition of excess isopropylamine. The toluene suspension was filtered and the solvent completely removed from the filtrate by rotary evaporation. The final product (0.33 g, 24%) was purified by using column chromatography with silica gel as the solid support and 1% MeOH/CH_2Cl_2 as the eluant. The appearance of the methylene ^{1}H resonance at 4.55 ppm (2H, s) and the chemical shifts vs TMS of both the toluidine aromatic resonances of the final product, 6.65 ppm (2H, d) and 7.01 ppm (2H, d), and the amino methyl resonance, 3.05 (3H, s), distinguish the final product from the amide-linked presursor. An additional toluidine resonance appears at 2.21 (3H, s), along with bipyridine resonances at 2.42 ppm (s, 3H), 7.15 ppm (m, 2H), 8.26 ppm (s, 1H), 8.31 ppm (s, 1H), 8.46 ppm (d, 1H), and 8.56 ppm (d, 1H). Anal. Calcd for $C_{20}H_{21}N_3O_3 \cdot 1.5H_2O$: C, 72.70; H, 7.32; N, 12.72. Found: C, 72.17; H, 6.64; N, 12.00.

[Re(dmb-tol)$(CO)_3$Cl] (1). This complex was prepared by using a standard procedure utilizing carbonyl displacement from $Re(CO)_5Cl$.[13] In a typical preparation, $Re(CO)_5Cl$ (0.21 g, 1.0 equiv) and dmb-tol (0.20 g, 1.2 equiv) were combined in 20 mL of dry toluene. The deaerated mixture was heated at reflux under Ar for 1.5 h. The yellow precipitate (0.34 g, 96%) was filtered and washed with ether. Anal. Calcd for $C_{23}H_{21}N_3O_3ClRe$: C, 45.35; H, 3.48; N, 6.82. Found: C, 45.04; H, 3.40; N, 6.90. IR spectrum: ν(CO) 2025, 1907, 1859 cm^{-1}.

^{1}H NMR (CD_3CN, ppm, vs TMS): δ 2.15 (s, 3H), δ 2.53 (s, 3H), δ 3.07 (s, 3H), δ 4.64 (s, 2H), δ 6.67 (d, 2H), δ 7.01 (d, 2H) δ 7.42 (m, 2H) δ 8.25 (s, 1H), δ 8.30 (s, 1H), δ 8.82 (d, 2H) δ 8.89 (d, 2H).

[Ru(4,4′-$(C(O)NEt_2)_2$bpy)$_2$(dmb-tol)]$(PF_6)_2$ (2). The complex Ru-[4,4′-$(C(O)NEt_2)_2$bpy]$_2Cl_2$ (40 mg, 4.3×10^{-5} mol) and dmb-tol (12 mg, 4×10^{-5} mol) were dissolved in an argon-sparged mixture of ethanol (5 mL) and H_2O (0.25 mL). The solution was heated at reflux under argon for 6 h, cooled to room temperature, and concentrated under vacuum. A saturated aqueous solution of KPF_6 was added, and the resulting orange precipitate was filtered and washed with H_2O and diethyl ether. The salt was purified initially with column chromatography (alumina, CH_2Cl_2/0.5% MeOH); yield = 30 mg, 53%. The product was eluted from the column as quickly as possible in order to avoid decomposition. Final purification was accomplished by using preparatory HPLC chromatography by utilizing linear gradient elution

(10) (a) Chen, P. Y.; Mecklenburg, S. L.; Meyer, T. J. *J. Phys. Chem.* **1993**, *97*, 13126. (b) Chen, P.; Mecklenburg, S. L.; Duesing, R.; Meyer, T. J. *J. Phys. Chem.* **1993**, *97*, 6811. (c) Chen, P.; Duesing, R.; Graff, D. K.; Meyer, T. J. *J. Phys. Chem.* **1991**, *95*, 5850. (d) Chen, P.; Duesing, R.; Tapolsky, G.; Meyer, T. J. *J. Am. Chem. Soc.* **1989**, *111*, 8305.

(11) Mann; Barnes. *Electrochemical Reactions in Nonaqueous Systems*; Bard, Ed.; Marcel Dekker Inc.: New York , 1970; pp 272−278.

(12) Elliott, C. M.; Hershenhart, E. J. *J. Am. Chem. Soc.* **1982**, *104*, 7519.

(13) Worl, L. A.; Duesing, R.; Chen, P.; Ciana, L. D.; Meyer, T. J. *J. Chem. Soc., Dalton Trans.* **1991**, 849.

(14) Sullivan, B. P.; Salmon, D. J.; Meyer, T. J. *Inorg. Chem.* **1978**, *17*, 3334.

(15) (a) Brown, H. C.; Narasimhan, S.; Choi, Y. M. *Synthesis* **1981**, 996. (b) Krishnamurthy, S. *Tetrahedron Lett.* **1982**, 23, 3315. (c) The borane adduct is described in ref 15a.

with 0−200 mM KBr in 1:3 (v/v) CH_3CN/H_2O. After elution, the complex was precipitated as the hexafluorophosphate salt by addition of a saturated aqueous KPF_6 solution followed by slow removal of acetonitrile under vacuum. Even after repeated HPLC purification, a small amount (<3%) of impurity was detected in the analytical HPLC. The amount of the impuritiy slightly increased after the second purification cycle. The observation that the impurity is formed during purification cycles indicates that the impurity is most likely an irreversible oxidative decomposition product of the toluidine. ^{1}H NMR (CD_2Cl_2, ppm, vs TMS): δ 1.18 (m, 24H), δ 2.2 (s, 3H), δ 2.51 (s, 3H), δ 3.04 (s, 3H), δ 3.42 (m, 16H), δ 4.67 (s, 2H), δ 6.64 (d, 2H, J = 8.6 Hz), δ 7.01 (d, 2H, J = 8.2 Hz), 7.34 (m, 2H), δ 7.4 (m, 4H), δ 7.55 (d, 1H, 5.8 Hz), δ 7.57 (d, 1H, J = 5.7 Hz), δ 7.78 (d, 2H, J = 5.7 Hz), δ 7.88 (d, 1H, J = 5.7 Hz), δ 7.9 (d, 1H, J = 5.7 Hz), δ 8.15 (s, 1H), δ 8.26 (s, 1H), δ 8.36 (s, 4H).

FABMS: M - $2PF_6$ (theoretical) = 1113.48, M - $2PF_6$ (sample) = 1113.4852 ΔM = 3.4 ppm. Mass-to-charge ratio: m/z (theoretical) = 556.74, m/z (sample) = 556.7

Measurements and Instrumentation. UV−visible spectra were measured in CH_3CN on a Hewlett-Packard 8452D diode array spectrophotometer. FT-IR spectra were recorded in KBr disks with a Mattson Galaxy Series FTIR 5020. ^{1}H NMR spectra were recorded on a Bruker WM250 spectrometer. Chemical shifts are reported as ppm vs TMS at 20 °C. FAB-MS measurements were obtained by using a JEOL HX110HF mass spectrometer at North Carolina State University. The resolving power was 10 000, the accelerating power was 10 keV, and the ion source temperature was 40 °C. HPLC purification was carried out by using cation exchange chromatography on a Brownlee CX-300 Prep 10 column. The elutions were controlled by a Rainin Dynamax SD-300 solvent delivery system equipped with 25 mL/min pump heads and monitored by a Shimadzu SPD-M10AV diode array UV−visible spectrophotometer fitted with a 4.5 mm path length flow cell. Elemental analyses were performed by Oneida Research Services.

The dmb-tol$^{\bullet+}$ radical cation was prepared in situ by stopped-flow mixing of separate CH_3CN solutions containing dmb-tol (1.2×10^{-4} M) and $(NH_4)_2Ce(NO_3)_6$ (2.4×10^{-4} M) at 25 °C, in a Hi-Tech Scientific Double Mixing stopped-flow mixing apparatus. Constant temperature was maintained by use of a Lauda RM6 circulating water bath. UV−visible kinetic measurements of the radical cation were made by use of a Hi-Tech CU-61 rapid scanning spectrophotometer attached to the stopped-flow mixing apparatus by using the KinetAsyst 2.0 software program. A total of 200 scans were collected over 1.5 s. An increase in absorption due to the radical cation (λ_{max} = 478 nm) appears within the first 15 ms. It disappeared completely within 1.5 s. The molar absorptivity of the radical cation was determined from the initial concentration of dmb-tol, assuming complete conversion. To test the latter assumption, a 10-fold excess of Ce(IV) was used, which gave no increase in the calculated concentration of radical cation.

Cyclic voltammograms collected at 100 mV/s were obtained in 0.1 M TBAH/CH_3CN solutions with a Princeton Applied Research 273 potentiostat/galvanostat interfaced to a personal computer. A silver/silver nitrate (0.1 M) reference electrode, a platinum wire auxiliary electrode, and a BAS MF-2013 platinum disk working electrode were used in a three-compartment cell. Solutions were deaerated by bubbling with N_2 for 10 min. Potentials were measured relative to the ferrocene couple (0.40 V vs SCE) and are reported vs SCE.[16]

All photophysical measurements were obtained in 1 cm path length quartz cells at 298 ± 2 K. Solutions for steady-state and time-resolved emission spectra were sparged with argon for 1 h prior to data collection. Solutions for transient absorption studies were subjected to six freeze−pump−thaw cycles under high vacuum.

Corrected steady-state emission spectra were recorded on a SPEX fluorolog photon-counting fluorimeter interfaced to a SPEX DM1B computer. The spectra were corrected for instrument response by the procedure supplied by the manufacturer. Emission quantum yields (ϕ_{em}) of optically dilute solutions (OD ~ 0.1 at the excitation wavelength) were measured relative to $[Ru(bpy)_3](PF_6)_2$ (ϕ'_{em} = 0.062) in CH_3CN.[17,18]

Emission lifetimes were measured by using a PRA nitrogen laser model LN 1000 and a PRA dye laser model LN102 combination for sample excitation. The emission was monitored at a right angle to the excitation source with a McPherson 272 grating monochromator and a Hamamatsu R928 PMT operating at 700 V. Transient absorption difference spectra were measured by using a Quanta Ray PDL-2 pulsed laser dye (Coumarin 460 dye) pumped by a Quanta-Ray DCR-2A Nd:YAG laser with an excitation pulse of ~6 ns at <5 mJ/ pulse. The excitation beam was coincident to an Applied Photophysics laser kinetic spectrometer, which utilized at 150 W pulsed Xe arc lamp as a probe beam, quartz optics, *f*/3.4 grating system, and a five-stage, cooled PMT. The outputs for both time-resolved experiments were collected with a LeCroy 7200A digital oscilloscope interfaced to a IBM PC. Time-resolved data were fit by utilizing a global minimization routine based on a modified Levenburg−Marquardt nonlinear, least-squares iterative procedure.

Results

Covalent attachment of *N*,*N*-dimethyltoluidine to 2,2′-bipyridine leads to a significant increase in the reduction potential, $E_{1/2}$ ($D^{+/0}$) = 0.86 V vs SCE in CH_3CN, relative to free *N*,*N*-dimethyltoluidine, $E_{1/2}$ ($D^{+/0}$) = 0.65 V. As has been previously reported in the literature, the radical cation is not sufficiently stable to prepare quantitatively by bulk electrolysis,[19] but cyclic voltammograms were chemically reversible at 100 mV/s with the ratio of anodic-to-cathodic peak currents ~1. Quantitative, in situ preparation was achieved by chemical oxidation with Ce(IV) by using rapid stopped-flow mixing. The absorption spectrum of the resulting dmb-tol$^{\bullet+}$ radical cation in CH_3CN has a visible absorption at λ_{max} = 478 nm, ϵ = 4200 M^{-1} cm^{-1}, and is similar to the literature spectrum for the *N*,*N*-dimethylaniline radical cation generated at low temperatures in an ethanol glass.[20] The ligand is stable in the solid state in air and in the absence of light for extended periods. Problems with irreversible decomposition of the Ru^{II} complex were encountered over extended periods in water.

Relevant ground-state and photophysical properties obtained in CH_3CN solution at 298 ± 2 K for [Re(dmb-tol)(CO)Cl], **1**, and $[Ru(4,4'\text{-}(C(O)NEt_2)_2bpy)_2(dmb\text{-}tol)]^{2+}$, **2**, are summarized in Table 1. ΔG°_{ES}, the free energy of the excited state above the ground state, was calculated from the emission spectra of $[Re(dmb)(CO)_3Cl]$ and $[Ru(4,4'\text{-}(C(O)NEt_2)_2bpy)_2(dmb)]^{2+}$ by application of a standard Franck−Condon analysis,[21] which gave ΔG°_{ES} = 2.58 ± 0.08 eV for the $Re^{II}(dmb^-)$ excited state and ΔG°_{ES} = 2.07 ± 0.06 eV for the $Ru^{III}(4,4'\text{-}(C(O)NEt_2)_2bpy^-)$ excited state.[21] From these values and the ground-state reduction potentials for $[Re(dmb)(CO)_3Cl]^{0/-}$ and $[Ru(4,4'\text{-}(C(O)NEt_2)_2bpy)_2(dmb\text{-}tol)]^{2+/+}$ couples in Table 1, $E^{\circ\prime}$ = 1.12 ± 0.1 V for the excited-state couple $[Re^{II}(dmb^-)(CO)Cl]^* + e^- \rightarrow [Re^{I}(dmb^-)(CO)Cl]^-$ and $E^{\circ\prime}$ = 0.88 ± 0.1 V for the excited-state couple $[Ru^{III}(4,4'\text{-}(C(O)NEt_2)_2bpy^-)(4,4'\text{-}(C(O)NEt_2)_2bpy)(dmb)]^{2+*} + e^- \rightarrow [Ru^{II}(4,4'\text{-}(C(O)NEt_2)_2bpy^-)(4,4'\text{-}(C(O)NEt_2)_2bpy)(dmb)]^+$.

(16) Connelly, N. G.; Geiger, W. E. *Chem. Rev.* **1996,** *96*, 877.

(17) Caspar, J. V.; Meyer, T. J. *J. Am. Chem. Soc.* **1983**, *105*, 5583.

(18) Emission quantum yields were calculated by the equation, $\phi_{em} = \phi'_{em}(I/I')(A'/A)$. I and I' are integrated emission intensities for the sample and a standard. A and A' are the absorbances at the excitation wavelength. ϕ'_{em} is the quantum yield of the standard, $[Ru(bpy)_3](PF_6)_2$, ϕ'_{em} = 0.062.[17]

(19) (a) Seo, E. D.; Nelson, R. F.; Fritsch, J. M.; Marcoux, L. S.; Leedy, D. W.; Adams, R. N. *J. Am. Chem. Soc.* **1966**, *88*, 3448. (b) Seo, E. T.; Nelson, R. F.; Fritsch, J. M.; Marcoux, L. S.; Leedy, O. W.; Adams, R. N. *J. Am. Chem. Soc.* **1967**, *89*, 447.

(20) (a) Williams, K. P. J.; Hester, R. E. *J. Raman Spectrosc.* **1981**, *10*, 161. (b) Chow, Y. L.; Danen, W. C.; Nelson, S. F.; Rosenblatt, D. H. *Chem. Rev.* **1978**, *78*, 243. (c) Kimura, K.; Yoshinaga, K.; Tsubomura, H. *J. Phys. Chem* **1967**, *71*, 4485.

Table 1. Electrochemical and Spectral Data in CH_3CN at 298 ± 2 K

complex or compound	($Re^{II/I}$ or $Ru^{III/II}$)	$E_{1/2}$(V)[a] $D^{+/0,b}$	$bpy^{0/-,c}$	UV−visible spectra λ_{max}, nm ($\epsilon \times 10^{-3}$, M^{-1} cm^{-1})[d]
dmb-tol		0.86		
[Re(dmb)$(CO)_3$Cl]	1.35		−1.44	364 (3.63); 290 (13.2); 254 (22.9)
[Re$(CO)_3$(dmb-tol)Cl]	1.45	0.91	−1.42	366 (2.99); 292 (13.3); 254 (23.0)
[Ru[4,4′-(C(O)NEt_2)$_2$bpy]$_2$(dmb)]$^{2+}$	1.39		−1.21	464 (12.8); 293 (64.6); 250 (37.8)
			−1.33	
[Ru[4,4′-(C(O)NEt_2)$_2$bpy]$_2$(dmb-tol)]$^{2+}$	1.35	0.89	−1.19	466 (14.8); 294 (68.0); 250 (49.8)
			−1.37	

[a] In 0.1 M TBAH vs SCE; ±0.05 V. [b] Potential for the $D^{+/0}$ couple localized on the toluidine donor. [c] Potential for the $bpy^{0/-}$ dmb-based couple for the Re complexes and 4,4′-(C(O)NEt_2)$_2$bpy-based for the Ru complexes. [d] ±2 nm, ±200 M^{-1} cm^{-1}.

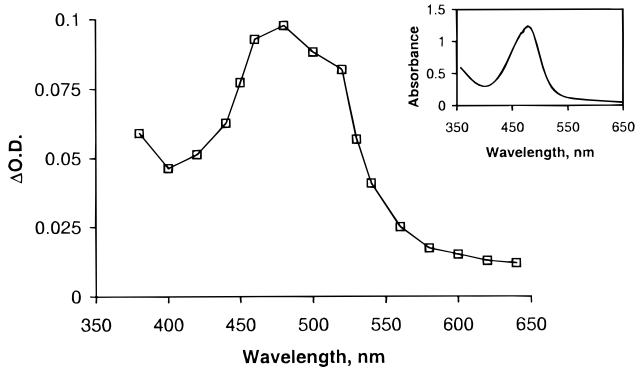

Figure 1. Transient absorption difference spectrum of [Re(dmb)-$(CO)_3$Cl] in CH_3CN at room temperature collected 10 ns after laser flash excitation at 355 nm at 2 mJ/pulse. Inset shows the ground-state absorption spectrum of the radical cation, dmb-tol^+, in CH_3CN generated chemically by oxidation with Ce^{IV} (see text).

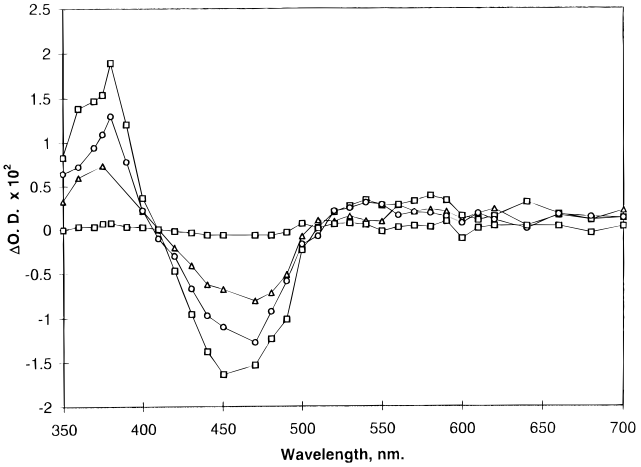

Figure 2. Transient absorption difference spectrum of [Ru[4,4′-(C(O)-NEt_2)$_2$bpy]$_2$(dmb)]$^{2+}$ in CH_3CN at 298 ± 2 K; excitation at 460 nm, 2.5 mJ/pulse, collected 10, 20, 30, and 60 ns after the laser pulse.

Compared to [Re(dmb)$(CO)_3$Cl], for which $\phi_{em} = 0.0058$, and $k(298 \pm 2\ K) = 2.0 \times 10^7\ s^{-1}$ ($\tau = 49$ ns) for excited-state decay,[13] emission from [Re(dmb-tol)$(CO)_3$Cl], **1**, is completely quenched with $\phi_{em} < 10^{-5}$. Transient absorption measurements following laser flash photolysis in CH_3CN ($\lambda_{exc} = 355$ nm, 2 mJ/pulse) reveal the appearance of a transient formed within the laser pulse (<5 ns) which is characterized by a new absorption feature centered at 480 nm, Figure 1. Time resolution of the transient decay based on measurements from 370 to 640 nm gave $k(298 \pm 2\ K) = (1.05 \pm 0.01) \times 10^7\ s^{-1}$ ($\tau = 95 \pm 1$ ns), independent of monitoring wavelength.

For [Ru(4,4′-(C(O)NEt_2)$_2$bpy)$_2$(dmb)]$^{2+}$ in CH_3CN, emission is observed at 653 nm, which decays with $k(298 \pm 2\ K) = 1.0 \times 10^6\ s^{-1}$ ($\tau = 997$ ns). In contrast to **1**, some emission is observed from [Ru(4,4′-(C(O)NEt_2)$_2$bpy)$_2$(dmb-tol)]$^{2+}$ **(2)**, centered at 664 nm, whose intensity varies somewhat with sample purification procedures, but typically with $\phi_{em} \sim 0.006$. The decay of this emission can be fit to the biexponential function, $I(t) = a \exp(k_1 t) + (1 - a) \exp(k_2 t)$, with $k_1 = (9.1 \pm 0.2) \times 10^5\ s^{-1}$ and $k_2 = (3.8 \pm 0.2) \times 10^7\ s^{-1}$. I_0 is the emission irradiance at $t = 0$. Transient absorption measurements conducted in CH_3CN ($\lambda_{exc} = 460$ nm, 2.5 mJ/pulse) gave the difference spectrum shown in Figure 2. The decay kinetics monitored at 380 and 480 nm were exponential and gave $k(298 \pm 2\ K) = (3.8 \pm 0.2) \times 10^7\ s^{-1}$, $\tau = 26 \pm 2$ ns. In the difference spectrum at 10 ns there appears to be a slight distortion at 450−420 nm due to light scattering from the 460 nm excitation pulse.

Discussion

Based on the photophysical data, $Re^I \rightarrow$ dmb metal-to-ligand charge transfer in [Re^I (dmb-tol)$(CO)_3$Cl] **(1)** is followed by rapid, essentially complete toluidine $\rightarrow Re^{II}$ intramolecular electron-transfer quenching. Quenching occurs within the time resolution of the apparatus used (<5 ns). Evidence for the formation of the ligand-based, redox-separated state, [Re^I-(dmb^--tol^+)(CO)Cl], appears in the transient absorption difference spectrum in the absorption feature at $\lambda_{max} = 478$ nm. This feature coincides with the absorption maximum for dmb-$tol^{\bullet+}$ generated by Ce^{IV} oxidation (Figure 1).

These observations are consistent with the sequence of reactions in Scheme 1 which occur following MLCT excitation. In the scheme, $Re^I \rightarrow$ dmb flash photolysis is followed by rapid ($k > 2 \times 10^8\ s^{-1}$) tol $\rightarrow Re^{II}$ electron transfer to give the redox-separated state, [Re^I(dmb^--tol^+)(CO)Cl]. Based on the excited-state reduction potential for [Re^I(dmb^-)(CO)Cl]*, estimated by emission spectral fitting,[21] this reaction is favored by ∼0.25 eV. The approximate free energy of the redox-separated state,

(21) A standard Franck−Condon analysis was applied to the emission spectra as described elsewhere.[13,22] The single mode approximation was used in the fits. For the Ru complex, $\hbar\omega$ was fixed at 1300 cm^{-1}.[22] For the Re complex, $\hbar\omega$ was fixed at 1450 cm^{-1}.[13] These are average values reflecting the contributions of a series of ν(bpy) ring stretching modes from 1000 to 1650 cm^{-1} with $\hbar\omega = \sum_j S_j \hbar\omega_j / \sum_j S_j$. The S_j and $\hbar\omega_j$ are the electron-vibrational coupling constants and quantum spacings for the contributing vibrations, j.[22,23] The other parameters in the fits were $S = \sum_j S_j$, E_0, the energy difference between the ground and excited states in their lowest vibrational levels, and $\Delta\bar{\nu}_{1/2}$, the bandwidth at half-maximum. The term $\Delta\bar{\nu}_{1/2}$ includes the solvent reorganizational energy (λ_o) and coupled low-frequency modes treated classically ($\lambda_{i,L}$) with $(\Delta\bar{\nu}_{1/2})^2 = (16 k_B T \ln 2)\lambda_{o,L}$, $\lambda_{o,L} = \lambda_o + \lambda_{i,L}$. The free energy of the excited state above the ground state, ΔG°_{ES}, was calculated from $\Delta G^\circ_{ES} = E_0 + (\Delta\bar{\nu}_{1/2})^2/(16 k_B T \ln 2)$. For [Re(dmb)(CO)Cl], $E_0 = 16\,400$ cm^{-1}, $S_M = 1.2$, and $\Delta\bar{\nu}_{1/2} = 3200$ cm^{-1}. For [Ru[4,4′-(C(O)NEt_2)$_2$bpy]$_2$(dmb)]$^{2+}$, $E_0 = 15\,500$ cm^{-1}, $S = 1.1$, and $\Delta\bar{\nu}_{1/2} = 1700$ cm^{-1}. Estimated errors are E_0 (± 5%), S (±10%), and $\Delta\bar{\nu}_{1/2}$ (±15%). These parameters are strongly correlated in their influence on the calculated band shapes. Appropriate combinations of parameters calculated in the ranges cited gave reasonable fits, but ΔG°_{ES} (±3%) was relatively well-defined.

Scheme 1

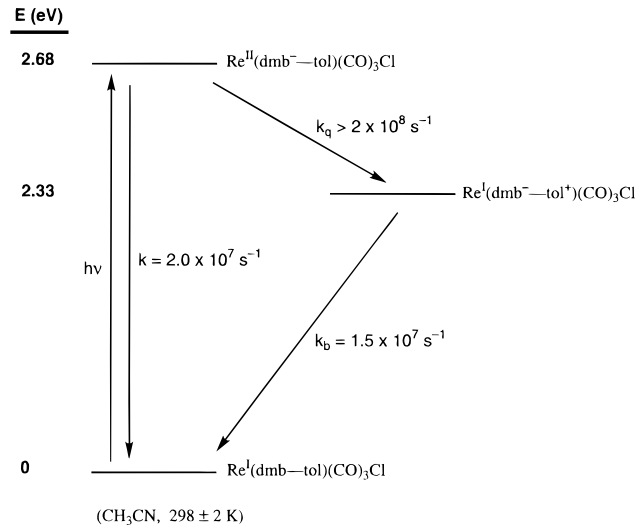

estimated from the ground-state redox potentials (Table 1) neglecting work terms, is 2.33 eV.

Photophysical events that occur following 456 nm MLCT excitation of $[Ru(4,4'\text{-}(C(O)NEt_2)_2bpy)_2(dmb\text{-}tol)]^{2+}$ **(2)** are more complex. In **2**, a small amount of residual emission is observed which could be fit to biexponential decay kinetics. In these fits there is evidence for a small amount of a long-lived ($\tau = 1.06\ \mu s$) emitting impurity which is present in varying amounts depending on sample purification. The remaining emission is intrinsic with $\tau = 26$ ns ($k = 3.8 \times 10^7\ s^{-1}$) and coincides with the kinetics obtained for decay of the transient observed by transient absorption measurements. The greatly decreased MLCT lifetime is consistent with intramolecular quenching analogous to that for the Re complex. The transient absorption difference spectrum in Figure 2 reveals the formation of a MLCT excited state having a bleach at ~470 nm, which coincides with the ground-state absorption maximum, and a characteristic absorption in the $\pi \rightarrow \pi^*$ region at 380 nm.[24] Given the electron-withdrawing character of the amide ligand and transient infrared results on the diethylester analogue, $[Ru(4,4'\text{-}(CO_2Et_2)_2bpy)_2(dmb)]^{2+}$, this is a $Ru^{III}(4,4'\text{-}(CO_2Et_2)_2bpy^-)$-based MLCT state.[25]

The bleach for the MLCT state at ~470 nm overlaps the absorption maximum for dmb-tol$^{\bullet+}$ at 476 nm ($\epsilon = 4200\ M^{-1}\ cm^{-1}$), is far more intense, and would mask the appearance of the radical cation. In addition to absorption by the radical cation, the redox-separated state, $[Ru^{II}(4,4'\text{-}(CO_2Et_2)_2bpy)(4,4'\text{-}(CO_2Et_2)_2bpy^-)(dmb\text{-}tol^+)]^{2+}$, would also exhibit a more intense ($\epsilon \sim 16\,000\ M^{-1}\ cm^{-1}$) $Ru^{II} \rightarrow (4,4'\text{-}(C(O)NEt_2)_2bpy)$ absorption that would be significantly red-shifted ($\lambda_{max} > 530$ nm) relative to the ground state, owing to the electron-donating ability of the reduced bipyridine.[26] If this feature were present to a significant degree, its overlap with the MLCT bleach would cause a blue shift in the maximum of the bleach, relative to the ground-state absorption maximum. The absence of these features in the transient absorption difference spectrum indicates that relatively little of the redox-separated state is present at equilibrium (<10%).

The dominance of the MLCT state and relatively low concentration of the redox-separated state are not surprising from a thermodynamic view. From emission spectral fitting on $[Ru(4,4'\text{-}(C(O)NEt_2)_2bpy)_2(dmb)]^{2+}$*, the energy of the $Ru^{III}(4,4'\text{-}(CO_2Et_2)_2bpy^-)$ MLCT state for **2** in CH_3CN is 2.07 eV. From the results of the electrochemical studies in Table 1, the energy of the ligand-based, redox-separated state, $(4,4'\text{-}(CO_2Et_2)_2bpy^-)(dmb\text{-}tol^+)$, is ~2.08 eV, neglecting work terms. On the basis of this analysis, $\Delta G^\circ \sim 0$ for the interconversion between the MLCT and the redox-separated state (RSS). Given these values, it is reasonable to expect that the two states coexist or that the RSS lies slightly higher in energy. This is consistent with the transient absorption results, from which it is estimated that [RSS]/[MLCT] < 0.1.

A summary of the photophysical events that occur in $[Ru(4,4'\text{-}(C(O)NEt_2)_2bpy)_2(dmb\text{-}tol)]^{2+}$ following $Ru^{II} \rightarrow (4,4'\text{-}(C(O)NEt_2)_2bpy)$ excitation is given in Scheme 2. On the basis of the available data the following comments can be made: (1) The lifetime of the initially formed MLCT excited state decreases from 995 ns ($k = 1.0 \times 10^6\ s^{-1}$) for the model complex $[Ru(4,4'\text{-}(C(O)NEt_2)_2bpy)_2(dmb)]^{2+}$* to $\tau_{em} = 26$ ns ($k = 3.8 \times 10^7\ s^{-1}$) in $[Ru(4,4'\text{-}(C(O)NEt_2)_2bpy)_2(dmb\text{-}tol)]^{2+}$*. The decrease is because of intramolecular toluidine $\rightarrow Ru^{III}$ reductive quenching. (2) The MLCT state lies lower in energy, and after initial quenching, an equilibrium is established between the redox-separated and MLCT states, which favors the latter. (3) The kinetics of excited-state decay are independent of monitoring λ, which demonstrates that the MLCT $\rightleftarrows$ RSS equilibrium is maintained rapidly compared to k_1, k_3. This is consistent with the kinetic limit k_2, $k_{-2} \gg k_1$, k_3 in Scheme 2. (4) Decay is dominated by the RSS and $k_3 \gg k_1$. In this limit, k_{obs} for excited-state decay becomes $\tau^{-1} = k_{obs} = k_3(k_2/k_{-2}) = k_3K_{eq}$, with $K_{eq} = [RSS]/[MLCT]$. On the basis of this analysis and $K_{eq} < 0.1$, $k_3 > 4 \times 10^8\ s^{-1}$, and k_2, $k_{-2} > k_3$.

With the new donor ligand dmb-tol, facile reductive quenching of the lowest MLCT excited states of $[Re(dmb\text{-}tol)(CO)_3Cl]$ and $[Ru(4,4'\text{-}(C(O)NEt_2)_2bpy)_2(dmb\text{-}tol)]^{2+}$ occurs. The radical cation has a characteristic spectroscopic signature at 478 nm ($\epsilon = 4200\ M^{-1}\ cm^{-1}$). Aniline derivatives as electron donors offer greater flexibility in the design of polypyridyl-based electron-transfer molecular assemblies, as compared, for example, to more commonly used PTZ derivatives. With the aniline derivatives, fine-tuning of the $D^{+/0}$ reduction potential in molecular assemblies can be achieved by varying the aniline substituents. Thus, the synthetic procedure for preparation of dmb-tol, generalized to phenyl-substituted anilines, opens the possibility of preparing a family of electron-transfer donors having a wide range of reduction potentials and systematic variation in the driving force for electron transfer.

The rate constant for $dmb^-\text{-}tol^+ \rightarrow$ dmb-tol back electron transfer in $[Re(dmb\text{-}tol)(CO)_3Cl]$, which interconverts the RSS and ground states, is enhanced relative to analogous PTZ electron transfers. For example, the rate constant for back electron transfer in the RSS of **1** is $1.05 \times 10^7\ s^{-1}$ with $\Delta G^\circ = -2.33$ eV. For the PTZ analogue, $[Re(dmb\text{-}PTZ)(CO)_3Cl]$, in CH_3CN under the same conditions, the rate constant for $dmb^-\text{-}PTZ^+ \rightarrow$ dmb-PTZ back electron transfer in the redox-separated state is slower ($k_b = 7.0 \times 10^6\ s^{-1}$), with $\Delta G^\circ = -2.21$ eV.[10a]

(22) (a) Kober, E. M.; Caspar, J. V.; Lumpkin, R. S.; Meyer, T. J. *J. Phys. Chem.* **1986**, *90*, 3722. (b) Caspar, J. V.; Meyer, T. J. *Inorg. Chem.* **1983**, *22*, 2444.
(23) (a) Dallinger, R. F.; Woodruff, W. H. *J. Am. Chem. Soc.* **1979**, *101*, 4391. (b) McClanahan, J.; Dallinger, R. F.; Holler, F. J.; Kincaid, J. R. *J. Am. Chem. Soc.* **1985**, *107*, 4853. (c) Danzer, G. D.; Janusz, A. G.; Strommen, D. P.; Kincaid, J. R. *J. Raman Spectrosc.* **1990**, *21*, 3.
(24) Lachish, U.; Infelta, P. P.; Gratzel, M. *Chem. Phys. Lett.* **1979**, *62*, 317.
(25) Chen, P.; Omberg, K. M.; Kavaliunas, D. A.; Treadway, J. A.; Palmer, P. A.; Meyer, T. J. *Inorg. Chem.* **1997**, *36*, 954.
(26) (a) For example, $[Ru(bpy)_3]^+$ has a $Ru^{II} \rightarrow$ bpy, MLCT absorption centered at 520 nm, with $\epsilon = 16\,800\ M^{-1}\ cm^{-1}$ (Maestri, M.; Gratzel, M. *Ber. Bunsen-Ges. Phys. Chem.* **1977**, *81*, 504).

Scheme 2

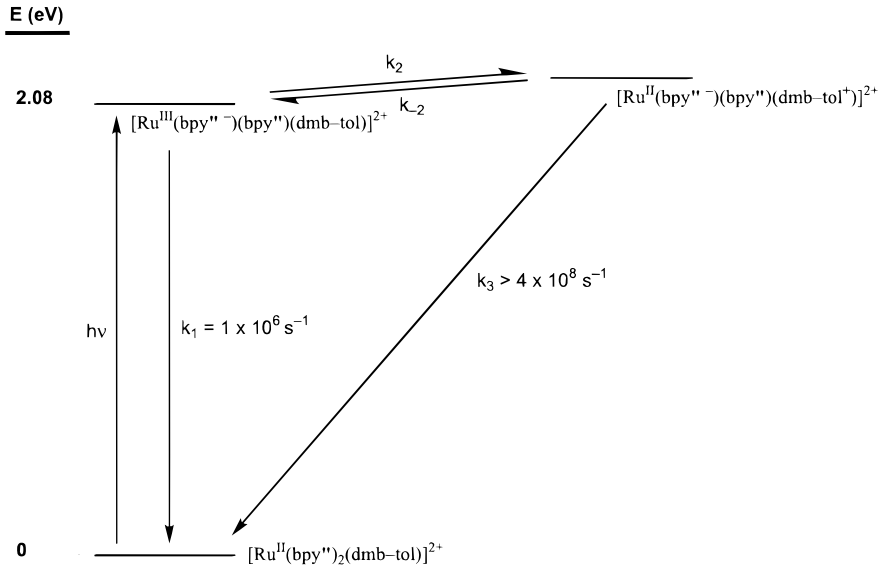

(CH_3CN, 298 ±2 K, bpy'' = 4,4'–$(C(O)NEt_2)_2$bpy)

These reactions occur deeply in the inverted region, and all other things being equal, k_{ET} is expected to decrease with increasing $-\Delta G°$. A detailed investigation of factors governing rate constant differences between aniline and phenothiazine derivatives is currently under way.

Acknowledgment. T.J.M. acknowledges the National Science Foundation for financial support under Grant CHE -9705724. C.M.P. also acknowledges the National Science Foundation for a Career Advancement Award and a Visiting Professorship Award for Women (Grant HRD-9627180) and Ithaca College for a leave of absence. Mass spectra were obtained at the Mass Spectrometry Laboratory for Biotechnology at North Carolina State University. Partial funding for the Facility was obtained from the North Carolina Biotechnology Center and the National Science Foundation.

IC980544Q